

Development of Pedestrian Detection System Using Far-Infrared Ray Camera

Hiroaki SAITO*, Takeshi HAGIHARA, Kenichi HATANAKA and Takanori SAWAI

Driver assistance systems that can detect pedestrians are increasingly being developed for the purpose of preventing road accidents. Far-infrared ray (FIR) cameras, which offer thermographic images, are useful for detection of pedestrians, but can be very expensive. To solve this problem, the authors had developed a low-cost FIR camera whose lenses are made of sintered polycrystalline zinc sulfide (ZnS), and also an algorithm for detecting pedestrians. This camera was originally developed for nighttime use, but this time the authors have developed a new pedestrian detection algorithm for detecting pedestrians at daytime and in bad weather. In this paper, the authors present the newly developed FIR camera and the new pedestrian detection algorithm.

1. Introduction

Driver assistance systems are being developed by automakers as mean to reduce traffic accidents. For examples, night vision systems that warn drivers of pedestrians during nighttime driving and pre-crash safety systems for collision mitigation have been commercialized in recent years, indicating that pedestrian detection will become an important function for driver assistance systems in the near future.

Use of far-infrared ray (FIR) cameras, which offer thermographic images, is expected to improve the performance of nighttime pedestrian detection. The authors had developed FIR cameras using low cost ZnS lenses, and also developed an algorithm for detecting pedestrians during nighttime. In this paper, the authors propose a new algorithm which aims to detect pedestrians not only in the nighttime but also in the daytime and in bad weather. The paper also describes a comparison of pedestrian detection sensors, an overview of the developed FIR camera, the details of the new pedestrian detection algorithm, and the results of the tests carried on urban roads.

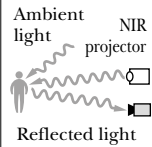
2. Far-infrared ray (FIR) camera

Table 1 shows a comparison of sensors for pedestrian detection. Millimeter-wave radars and laser radars used in collision mitigation systems are not included in the table because these radars are difficult to distinguish pedestrians from other objects such as cars. FIR cameras can measure the “temperature” of pedestrians, an example of FIR images is shown in Fig. 1. In general, FIR cameras are said to have the following advantages and disadvantages. The FIR images in bad weather and at daytime are shown in Fig. 2 and Fig. 3, respectively.

(a) Advantages:

- FIR cameras can detect pedestrians in bad weather better than other cameras because far-infrared rays are

Table 1. Comparison of sensors for pedestrian detection

		Far-infrared-ray (FIR) camera	Near-infrared-ray (NIR) camera	Visible-ray camera
Detection principle		Detects the far infrared ray (temperature) from the object Detectable frequency bandwidth: 8-12 um 	Detects the ambient light or reflected light using the projector system (only at nighttime) Detectable frequency bandwidth : 0.8-1.1 um 	Detects the ambient light or reflected light from the headlight Detectable frequency bandwidth: 400-700 nm
	Performance	Day	Good	Good
	Night	Excellent	Good	Poor
	Bad weather	Good	Poor	Poor

less susceptible to moisture than rays of other wavelength bands.

- Unlike near-infrared-ray (NIR) or visible-ray cameras, FIR cameras are susceptible to disturbing light, such as oncoming headlights.

(b) Disadvantages:

- In the daytime, there is little temperature difference between pedestrian and background objects (such as buildings and roads) because the sun heats background objects.

- FIR cameras are more expensive (lenses and imaging devices are especially expensive) than NIR cameras or visible-ray cameras.

Section 3 describes the newly developed pedestrian detection algorithm for daytime and bad weather, and gives experimental results.



Fig. 1. FIR image at nighttime



Fig. 2. FIR image in rainy weather



Fig. 3. FIR image at daytime

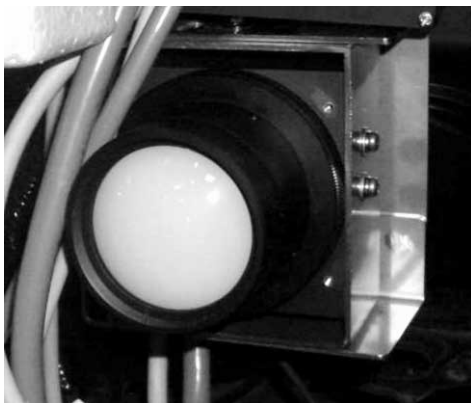


Fig. 4. Developed FIR camera

The newly developed FIR camera is shown in **Fig. 4**. This camera uses lenses that are made of sintered polycrystalline zinc sulfide (ZnS). The optical characteristics such as refractive index and transmittance of ZnS are inferior to those of germanium, which is a typical material for FIR lenses, but the authors improved the optical design of ZnS lens to achieve sufficient optical performance. Because ZnS lenses have lower material and production costs than germanium lenses, the use of ZnS lenses reduces the total cost of FIR camera. **Table 2** shows the specifications of the developed FIR camera.

Table 2. Specifications of developed FIR camera

	Specifications
Field of View	12×9 degrees
Number of Pixels	320×240 pixels
Intensity Resolution	8 bits
Camera Size	H80×W80×D100 mm
Image Output Format	NTSC

3. Pedestrian detection algorithm

The process flowchart of the newly proposed pedestrian detection algorithm is shown in **Fig. 5**. In many cases of nighttime pedestrian detection, processing methods based on image binarization are used because the intensity (i.e. temperature) of pedestrians is higher than that of background objects. However, at daytime or in bad weather, making assumptions on the intensity is not always effective because of environmental influences on FIR images (**Table 3**). The authors therefore tried to find alternative effective conditions, and found that the “contours” of pedestrians and background objects are less influenced by weather conditions and time of the day. Based on this finding, the authors have developed a new pedestrian detection algorithm composed of three processes, which are contour-based extraction, tracking, and classification of candidate areas. These processes are explained in details in the following sections.

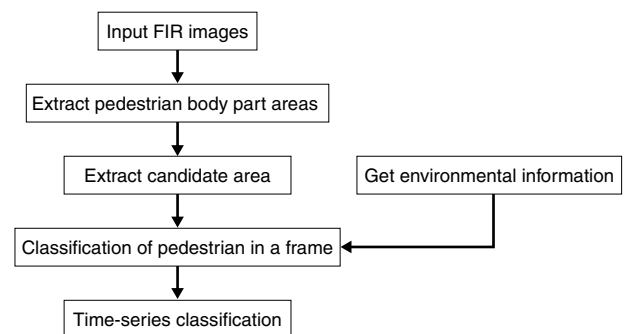


Fig. 5. Process flowchart of developed pedestrian detection algorithm

Table 3. Features of FIR images

Scene	Night (fine or cloudy weather)	Day	Bad weather
Image example			
Features of FIR image	<ul style="list-style-type: none"> · Pedestrian intensities are usually higher than background intensities. · Object contours are clear. 	<ul style="list-style-type: none"> · Pedestrian intensities are usually lower than background intensities (influence of the sun). · Object contours are clear. 	<ul style="list-style-type: none"> · Pedestrian intensities are usually higher than background intensities (due to decreased object temperatures). · Object contours are not clear (due to water drops on camera lenses).

3-1 Contour-based candidate area extraction

The method of contour-based candidate area extraction uses the intensity difference between a pedestrian and the background and a constrained condition of distances to pedestrian body parts. The constrained condition is based on the assumption that the distance between FIR camera and each pedestrian body part (head, arms, torso, and legs) is the same. However, the contour of a pedestrian is not always a continuous line and is usually disconnected at every parts of the body. Therefore, the candidate area extraction method is made of two steps: (1) Extraction of body part areas, and (2) grouping of body part areas, as shown below.

(a) Extraction of pedestrian body part areas

First, the contours of the pedestrian and the background are extracted from the FIR image (**Fig. 6**). In consideration of the cases of bad weather where blurred images are obtained, the Prewitt operator is used so that smooth contours can be extracted. Next, neighboring contour points are connected and contour groups are constructed. The reason of this process is to prevent the occurrence of errors at the following disparity segmentation process. The constructed contour groups may include the contour points that belong to different objects, so a contour group is divided into several blocks (ex. 4x4 pixels, **Fig. 7**), and then reconstructed after being judged whether or not these blocks belong to the same object. In the judgment process, each block's disparity (depends on the distance from FIR camera, as shown in **Fig. 8**) is calculated by using stereo cameras, and the blocks subjected to below conditions are classified into the same group.

- Disparity difference between the blocks are within a certain range.
- Blocks belonged to the same contour group before being divided.

The last step of body part area extraction is the expansion of contour groups. Contour points may not always be extracted on all boundaries between pedestrian and background, so the areas of contour groups need to be expanded to the areas that belong to pedestrian

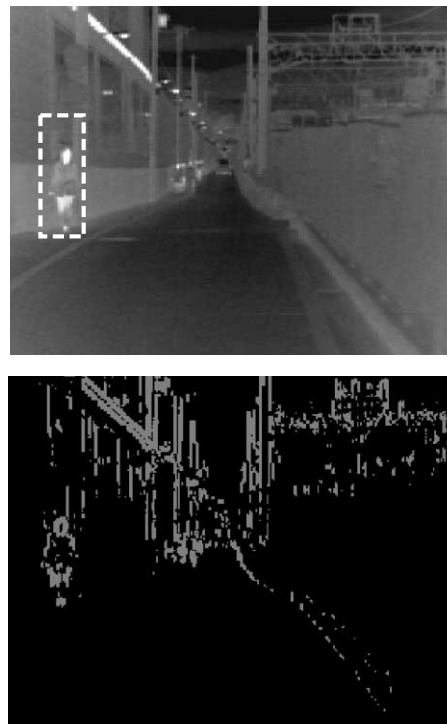


Fig. 6. Extracted contours (Prewitt operator)

and do not involve contour points. The expansion process has three steps: a) Set the blocks around the contour group area, b) calculate the disparity of each block, and c) unite the block with the contour group if the block has the disparity that is nearly equal to that of the contour group.

(b) Grouping of pedestrian body part areas

After the pedestrian body part areas were extracted, the body part areas are grouped to extract the candidate area, which is equal to the entire body of the pedestrian. This process has two steps: Unitizing and proving. In the unitizing process, the pedestrian body part areas of equal disparity are unitized and the candidate area is generated (**Fig. 9**). Next, in the proving process, the

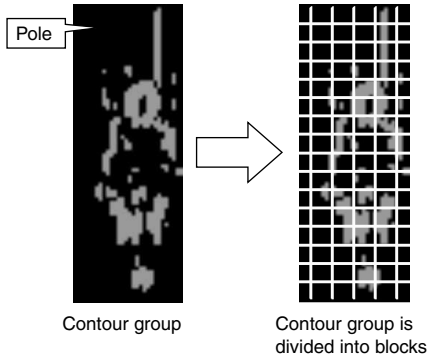


Fig. 7. Dividing of contour group

spatial disparity among the body part areas in the candidate area are calculated, and judged whether or not it is equivalent to the spatial disparity of the surrounding areas. The reason this process is performed is that some candidate areas may consist of “several” objects which are adjacent to each other and have disparities that are nearly equal. Therefore, if the spatial disparity of the body part areas is different from that of the surrounding areas, the candidate area is divided into parts before being unitized.

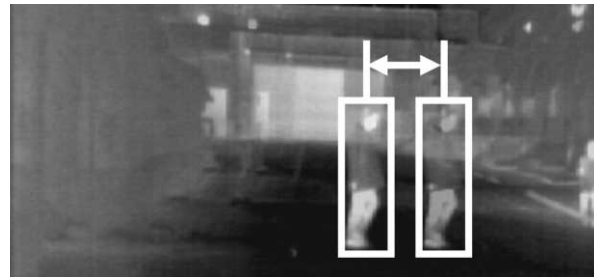
3-2 Candidate area tracking

Candidate areas are tracked over time so that candidate area classification can be performed as described in Section 3-3. In the candidate area tracking process, the similarity between the candidate areas in the current and last frames is calculated. If the similarity is larger than a certain level, then these candidate areas are labeled as the same. In calculating the similarity, parameters such as candidate area size variation and gravity difference are used. In addition, when the difference of gravity is calculated, the coordinates of the candidate area are corrected by calculating the yaw and pitch angles of the car.

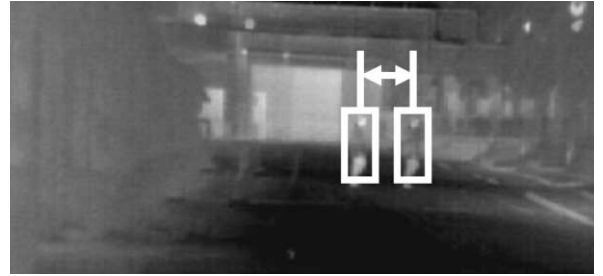
3-3 Candidate area classification

Candidate area classification is a process of judging whether or not the extracted candidate area is a pedestrian. In order to reduce the occurrence of classification errors due to occlusion or video noise, this process consists of two steps: The current frame classification and the time-series classification, as shown below.

(a) Classification in current frame



A) Point-to-point topology



(b) Pedestrian 80m away

Fig. 8. Dividing of contour group

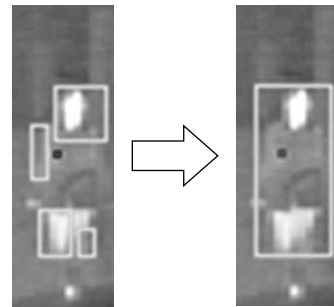


Fig. 9. Grouping of body part areas using disparity information

First, each candidate area is divided into several body part areas, such as head and legs, and the “plausibility” is calculated for each body part area. The candidate area is judged whether or not it is a pedestrian using the calculated plausibility. Then, in consideration of the variation of images due to weather and time of the day, the judgment is performed in accordance with environmental conditions. For example, when extracting a head area at nighttime or in bad weather, image binarization is used because a head usually has a higher intensity than the background. However, this method is not useful in the daytime because the sun heats the background and the intensity of the head area decreases. Therefore, the head area extraction using image binarization is performed only at nighttime or in bad weather (Fig. 10), and at daytime the head contour consisting of contour points is used. Parameters such as binarization threshold are derived statistically in consideration of environmental conditions.

(b) Time-series classification

This process uses the results of classification in cur-

rent and past frames, using the tracking process shown in Section 3-2. A candidate area is judged as a “pedestrian” only when the ratio of the frames the candidate area is judged as a “pedestrian” in total frames exceeds a certain value.

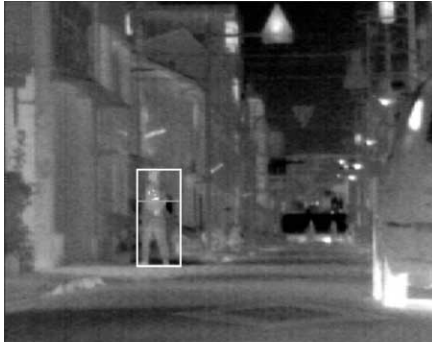


Fig. 10. Result of head area extraction

4. Experimental results

To validate the effectiveness of the newly proposed pedestrian detection algorithm, the authors evaluated the performance of this algorithm in urban roads at daytime and in bad weather, and compared the performance results to those at nighttime (evaluation conditions are shown in Table 4).

Table 4. Evaluation conditions

No	Environmental conditions	Remarks
1	Day (fine or cloudy weather)	Temperature : 15-35 [degrees Celsius] Amount of solar radiation : 1.5-2.8 [MJ/m ²]
2	Day (rainy weather)	Temperature : 20-27 [degrees Celsius] Amount of precipitation : 0-5 [mm/h]
3	Night (rainy weather)	Temperature : 20-25 [degrees Celsius] Amount of precipitation : 0-5 [mm/h]
4	Night (fine or cloudy weather)	Temperature : 7-30 [degrees Celsius]

*The “amount of solar radiation” values are referenced from the Japan Meteorological Agency JMA (<http://www.data.jma.go.jp/>)
*The evaluation video was recorded in Osaka area.

The detectable distance range is 20 to 50 m (horizontal angle 12 degrees) from the car, and the speed range of the car is within 60 km/h, according to the speed limit on public roads in Japan. Cases described below are exceptions because pedestrian detection is difficult.

a) Pedestrians are not visible by both cameras due to occlusion.

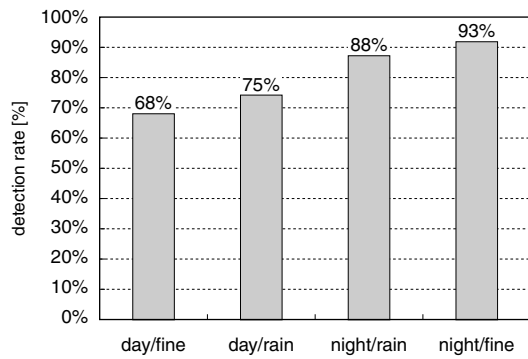
b) Car turned around at the crossing.

The experimental results are shown in Figure 11 and the details are described below.

(a) Daytime

The detection rate was 68%. This result represents that the performance of the developed algorithm is

Fig. 11. Pedestrian detection rate



unsatisfying for use in the detection of pedestrians. The authors made efforts to find the cause of low detection performance, and discovered that the contours of undetected pedestrians are poorly extracted because the intensities of both pedestrians and the background are saturated by the influence of auto offset control (AOC) of FIR cameras. Therefore, the detection rate can be elevated by adequately controlling the camera parameters. Figure 12 shows the detection result in the daytime.



Fig. 12. Pedestrian detection at daytime

(b) Bad weather

The detection rate is 75% to 88%. The developed algorithm can achieve relatively good performance. False detection may occur in the case where the contour of a pedestrian cannot be extracted because of blurring of images due to absorption and scattering of FIR caused by the water drops on the lenses. However, the contour can be partially extracted even when water drops exist on lens surfaces, so by elevating the modulation transfer function (MTF) of the lenses and the extracting the contour more clearly, better performance can be achieved. **Figure 13** shows the detection result in bad weather.

5. Conclusions

The authors have presented a new pedestrian detection system using a FIR camera, which employs ZnS lenses. And the performance of the detection algorithm was measured at daytime and in bad weather. The results indicated that the proposed pedestrian detection algorithm achieves a relatively good detection rate although the performance is not satisfying yet. It is considered that the proposed pedestrian detection system has a potential to detect pedestrians in all weather and any time of the day. In the future, the authors will try to improve the detection rate at daytime and achieve the function of self-adjusting the camera parameters.

References

- (1) Development of Night Vision System, HONDA R&D Technical Review, Vol.13, No.1, 2001
- (2) Development of Pedestrian Detection System at Nighttime, SEI Technical Review, Vol.169, 2006

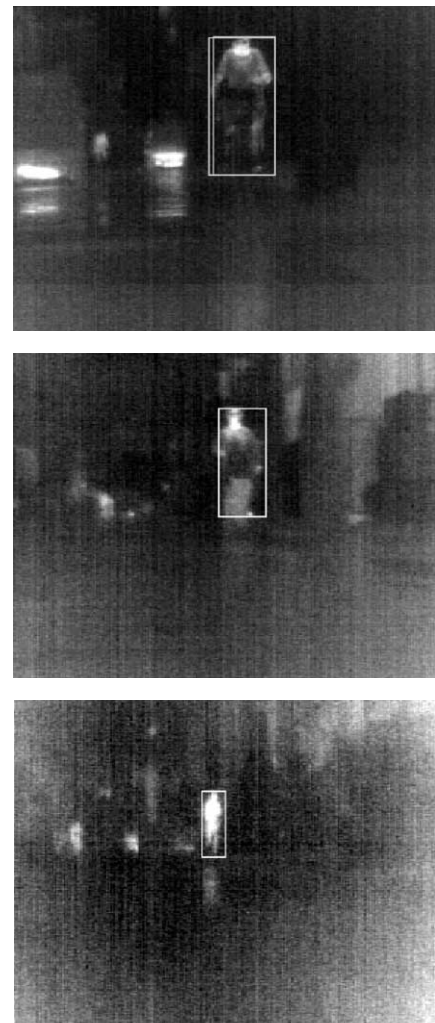


Fig. 13. Pedestrian detection in rainy weather

Contributors (The lead author is indicated by an asterisk (*)).

H. SAITO*

- Control & Communications Networks R&D Department, Automotive Technology R&D Laboratories

T. HAGIHARA

- Assistant Manager, Control & Communications Networks R&D Department, Automotive Technology R&D Laboratories

K. HATANAKA

- Manager, Control & Communications Networks R&D Department, Automotive Technology R&D Laboratories

T. SAWAI

- General Manager, Automotive Technology R&D Laboratories